Contour based Split and Merge Segmentation and Pre-classification of Zooplankton in Very Large Images

Enrico Gutzeit[1], Christian Scheel[2], Tim Dolereit[1] and Matthias Rust[3]

[1]*Fraunhofer Institute for Computer Graphics Research IGD, Joachim-Jungius-Str. 11, 18059 Rostock, Germany*
[2]*University of Rostock, Institute for Computer Science, Albert-Einstein-Str. 22, 18059 Rostock, Germany*
[3]*Arivis AG, Kroepeliner Str. 54, 18055 Rostock, Germany*

Keywords: Segmentation, Contour, Split & Merge, Pre-classification, Shape Features, Zooplankton, Large Images.

Abstract: Zooplankton is an important component in the water ecosystem and food chain. To understand the influence of zooplankton on the ecosystem a data collection is necessary. In research the automatic image based recognition of zooplankton is of growing interest. Several systems have been developed for zooplankton recognition on low resolution images. For large images approaches are seldom. Images of this size easily exceed the main memory of standard computers. Our novel automatic segmentation approach is able to handle these large images. We developed a contour based Split & Merge approach for segmentation and, to reduce the non-zooplankton segments, combine it with a pre-classification of the segments in reference to their shape. The latter includes a detection of quasi round segments and a novel one for thin segments. Experimental results on several large images show that we are able to handle them satisfactorily.

1 INTRODUCTION

Zooplankton and phytoplankton are a significant part of the food chain of every aquatic ecosystem. Consequently, they represent a fundamental parameter of the ecosystem's structure and act as an indicator of its structural changes. The analysis can be done in situ or in the laboratory with fixed and filtered plankton samples. Expected results are the identification of plankton in these samples and also their classification into the appropriate species categories. The usual approach starts with the deployment of plankton nets followed by manual evaluation of the gathered samples by a taxonomic expert. This is a labor intensive and time consuming procedure which heavily depends on rare expert knowledge. Hence, the automatic recognition of plankton is of growing interest in biology. Many good reasons for automatic plankton recognition are discussed by Gaston and O'Neill (Gaston and O'Neill, 2004). A full solution for an automatic or semi-automatic system should consist of an image acquisition stage (laboratory or in situ) followed by an image processing stage.

In this paper we concentrate on zooplankton samples acquired in a laboratory setup. We focus on the segmentation of zooplankton and briefly describe the image acquisition as well as the zooplankton recognition. Our acquisition method is realized with low cost equipment producing high resolution images in size of about 60000×60000 pixels with a pixel size of about 0.4 μm. Images of this size easily exceed the main memory of standard computers. Our following novel automatic segmentation approach is able to handle these large images. It comprises an adjusted segmentation of all the objects in the image and a pre-classification to eliminate non-zooplankton segments.

The paper is organized as follows. Section 2 presents related work and in section 3 the problems to solve are discussed. Our approach to image acquisition and image processing is explained in section 4. In section 5 we discuss our results and we finish with conclusions and future works in section 6.

2 RELATED WORK

The recognition and quantification process can be supported by different techniques. The approaches of (Sheldon and Parsons, 1967), (Fawell, 1976), (Herman and Dauphinee, 1980), for instance, do not involve image processing methods, but electronic, colorimetric or ultrasonic measuring methods. Image processing is a powerful tool for automatic recognition and classification of zooplankton. A typical analysis pipeline starts with the image acquisition and consists of segmentation, feature extraction, training and classification stages. Some first exam-

ples are the works of (Katsinis, 1979) or (Jeffries et al., 1984). Common shape features for classification are extracted from the threshold-segmented images of low resolution (256×256 px). The images in (Chehdi et al., 1986), taken through a microscope, are already slightly bigger (512×512 px). Our work concentrates on images many times larger and requires advanced methods for automatic segmentation.

More recent and also technically more mature approaches mostly contain a special imaging device in combination with a specific image processing system. Imaging devices can be specialized to work either in situ or in a laboratory. In situ devices are able to image flowing particles in a volume of water over time. They are mostly constructed as mooring buoy, towed body or as an installation on a ROV or AUV. A first example for an in situ device is the Video Plankton Recorder (VPR) (Davis et al., 1992). An identification Software, the Visual Plankton, to recognize plankton in images taken by the VPR is described in (Davis et al., 2005). The image acquisition is adjustable between a resolution of 10 *μm* and 300 *μm* per pixel. The segmentation is done after binarization and regions of interest (ROIs) are extracted. Another system is the Shadowed Image Particle Profiling Evaluation Recorder (SIPPER) (Samson et al., 2001) with the Plankton Image Classification and Extraction Software (P.I.C.E.S.) (Luo et al., 2004). Binary images with a pixel resolution of 50 *μm* are produced and hence, a segmentation is already given. The Underwater Vision Profiler (UVP) (Picheral et al., 2010) is suited for real-time, in situ particle counting, sizing and zooplankton detection (Website, 2013b). This is done by integrating a dedicated software within an intelligent camera, which is able to remove a background image. The pixel resolution of the images amounts to 174 *μm*. Further systems are the HAB-Buoy (Culverhouse et al., 2006) coupled to the Dinoflagellate Categorisation by Artificial Neural Network (DiCANN) software (Toth and Culverhouse, 1999), the In Situ Ichtyoplankton Imaging System (ISIIS) (Tsechpenakis et al., 2007; Tsechpenakis et al., 2008), the ImagingFlowCytobot (Olson and Sosik, 2007) and CytoBuoy (Dubelaar and Jonker, 2000).

In a laboratory setup, like our scenario, water samples can be prepared and analyzed. The commercial system Flow Cytometer And Microscope (Flow-CAM) (Sieracki et al., 1998) is equipped with the software Visual Spreadsheet (Website, 2013a). The software is able to extract sample particle sizes of 2 *μm* to 2 *mm* after segmentation and stores the ROIs. No details on the process are given. The system most comparable to ours is ZooScan (Gorsky and Gros-

jean, 2003) with the software Zooprocess and Plankton Identifier (Website, 2013c). Zooscan is a waterproof scanner with a maximal resolution of 2400dpi resulting in a pixel size of 10.6 *μm*. On Zooscan's website is stated: "if all available image dimensions can be acquired, there is still some limitation for the largest images processing. We are working on new macros that will overcome these limitations soon". In Zooprocess a background image is substracted to segment and extract individual objects. Zooprocess and Plankton Identifier are also able to process images from UVP.

Existing systems are *not* able to produce or handle large images as required in our scenario. Particularly, the published post-processing and segmentation algorithms require the images to fit into the computer's main memory.

3 DISCUSSION OF PROBLEMS

In our scenario, zooplankton species inside a counting chamber with water (diameter 25 *mm*) have to be recognized. Images of the chamber are taken stepwise by a microscope camera.
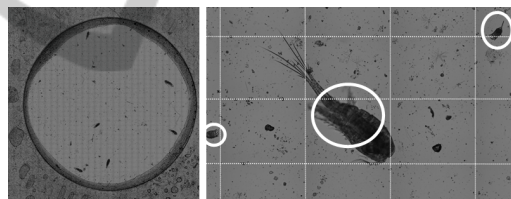

Figure 1: The counting chamber (left) and a part of it (right) with small and large species are shown. The stitched tiles are illustrated through lines and species with circles.

The images (tiles) are stitched together to a large image (approx. 60000×60000 px), which is illustrated in figure 1. The zooplankton is located only inside the counting chamber. Hence, it is helpful for further processing to detect the contour of this chamber. For recognition, a segmentation of the zooplankton is needed. The following problems must be solved to segment the zooplankton. Different zooplankton species can vary in size and in positioning. Some species can overlap multiple tiles due to a position on the border and large species can be even bigger than a single tile. On the contrary, small species can be similar in size of an unimportant particle (nonzooplankton). A further problem is the size of the image, which is too big for processing at once. Also, there are visible side effects after the stitching process due to illumination variances that lead to high gradients at the borders of the acquired tiles.

To overcome the problems we developed a contour based Split & Merge approach for segmentation. We do not split the image in homogenous regions and merge similar regions like in (Kelkar and Gupta, 2008). In our approach we split the image in regular tiles and merge the segmented contours in an iterative way. Furthermore, to reduce the non-zooplankton segments we implemented a pre-classification of the segments in reference to their shape. Our novel segmentation and pre-classification approach will be described in following section.

4 OUR APPROACH

Our approach to segment and pre-classify zooplankton is divided into five steps, which is illustrated in figure 2.
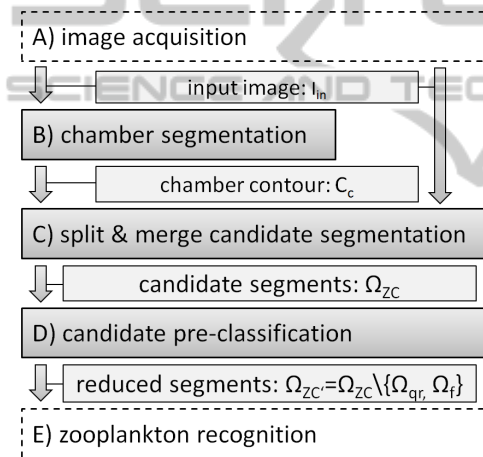

Figure 2: Our segmentation and pre-classification procedure for very large images.

In step A the images are acquired with an inverted dissected light microscope setup. The images are stitched together and post processed into a large grayscale input image. Thereafter, in step B, the contour of the counting chamber is detected to reduce the region to be processed in the following steps. The region inside the chamber is segmented in step C with a Split & Merge approach. As result we get segments representing zooplankton and non-zooplankton of different kinds. In step D we execute the pre-classification to simplify the recognition process. Thereby, we can reduce the non-zooplankton set in our scenario. Finally, a zooplankton recognition with a support vector machine (SVM) is done in step E. In this paper we set the focus on step B, C and D. An overview of the main notations used in this paper is given in table 1.

Table 1: Main notation used in this paper.

I_{in}	large grayscale input image
C, P	contour and point in general
C_c	the counting chamber contour
C_{zc}	a zooplankton candidate contour
C_{Ql}	a contour in a quadtree leaf
C^*, C^+	a complete and incomplete contour
Q, Q_l	quadtree, quadtree leaf
Q_{rb}	right and bottom quadtree neighbor
P_s, P_e	start and end contour merging point
Ω_{ZC}	zooplankton candidate segment set
Ω_{qr}, Ω_t	set of quasi round and thin segments
$\Omega_{ZC'}$	reduced set of zooplankton candidate

4.1 Image Acquisition

We used counting chambers with a glass bottom (Utermoehl, Kolkwitz) and an inverted dissected light microscope setup (Olympus IX50). Due to the required resolution and the thickness of the sample we added a motorized xyz-stage (Maerzhaeuser) to support tiled acquisition (xy) in multiple focus planes (z). Sufficient results were achieved with a $10\times$ magnification lens and a total number of 5 focus planes, which leads to a data size in the gigabyte range. The acquisition is controlled by the imaging software arivis Browser with an acquisition module that is connected to the microscope components and allows the definition of the required acquisition strategies and parameters. The single tiles are acquired as RGB images with a configurable overlap for compensating small variations in the motor stage positioning. After acquiring the single images an automated stitching and intensity compensation are performed to create a large plane from the single tiles. Color information is not utilized for subsequent steps, so all planes are converted to one greyscale plane. To further reduce the amount of data, an edge blending algorithm was applied that creates one merged image from the single focus planes by selecting pixels with the highest contrast.

4.2 Chamber Segmentation

Zooplankton is positioned only inside the counting chamber (see figure 1). For this reason, the detection of the chamber contour C_c is required. We have scaled the large image to a width of 2048 pixel. The following methods were implemented and tested for their ability to extract the contour of the counting chamber properly.

4.2.1 Longest Contour

The region inside the chamber is brighter and many edges are in the darker outside region. A contour seems to be directly calculable by binary segmentation and a strengthening of the edges. Firstly, a binary segmentation with Otsu's Method (Otsu, 1979) is performed on the image. After a gaussian smoothing a canny edge detection is applied, followed by some morphological operations. Finally, the longest contour in the resulting binary image is extracted.

4.2.2 Active Contours

The chamber is nearly round and enclosed by a contour with high gradients. However, there is much noise in the image leading to high gradients too. An active contour (Kass et al., 1988) applied on a preprocessed image seems to be appropriate. Therefore, we first perform a binary segmentation with Otsu's Method on a intensively smoothed image. After a morphological closing, a Hough transform for circle detection is used to determine the starting contour points. The active contour algorithm is executed on the binary image. We choose an equal weighting of the internal and external energy terms, without external constrains.

4.2.3 Region Growing

We also implemented a region growing approach, since the chamber is positioned at the image center, it is large in size and its region is even in brightness. Consequently, a seed point inside the chamber can be calculated reliably. We choose a center rectangular area of 5% of the image size and use the pixel with the lowest gray value as seed point. It can happen, that the pixel is enclosed by noise and the segmented region will get too small. In this case, different seed points are chosen in the rectangular area until the segmented region is bigger than 35% of the image. A general problem of region growing is leaking. Leaking is improbable in our case, because the chamber is surrounded by a darker area and there are high gradients from the inside to the outside area. After a successful region growing with a flood fill algorithm the longest contour is extracted. The resulting contour can have some unwanted protrusions, because of species or image artifacts nearby or on the chamber contour. We eliminate the protrusions by using our own polygon approximation. Therefore we analyze the angle changes of the contour points. Our elimination process works with two points P_1 and P_2. We use P_1 and P_2, an angle and a minimal/maximal distance from P_2 to span a searching area. The point in the

searching area with the shortest distance to the convex hull on the extracted contour is used as new point P_2. The old point P_2 is set to P_1. The process is repeated until the starting point is reached.

4.3 Contour based Split & Merge Candidate Segmentation

The input image I_{in} can be larger than the available main memory. Hence, we use a Split & Merge approach that first, splits the large image into smaller processable tiles and merges the results afterwards. Additionally, to compensate for the high gradients at the tile borders resulting from illumination variances during acquisition, we choose a tilesize that matches the size of the acquired tiles (including stitching parameters).
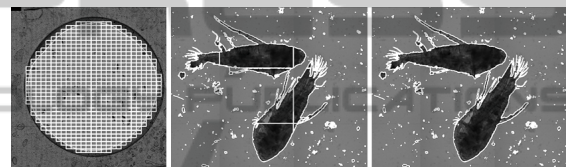

Figure 3: From left to right the leaf notes Q_l of the quadtree, not merged and merged contours of the zooplankton candidates are illustrated.

To process the large image data in a way that is structured and easy to handle, we make use of a quadtree data structure Q. The quadtree is used for splitting the image top down and managing the resulting tiles and their neighborhood. A quadtree node lying inside of or on the chamber contour C_c is further split, until a node has the size of a single tile (leaf node Q_l). Only the leaf nodes Q_l are processed further in our approach (see left in figure 3).

After the construction of Q, a segmentation and merging process is done, which will be described in the following subsections. A set of segments Ω_{ZC} is resulting and available for further processing in step D.

4.3.1 Tile segmentation

The segmentation is done separately for every quadtree leaf Q_l in Q. Zooplankton inside the grayscale tiles typically varies in shape and texture, but consists of pixels with similar high gray values. Hence, a simple and fast threshold segmentation is appropriate. A single threshold is used for all tiles to avoid unaligned fragments in the case of specimen located on tile borders. The threshold is determined on the whole input image I_{in} by Otsu's Method. To reduce the influence

of noise, the image is smoothed and a binary segmentation followed by a morphological filtering (closing and opening) is performed. If a tile in Q_l is overlapping the chamber contour C_c, then the irrelevant outside contours are removed. Finally, all the contours of the remaining segments C_{Ql} are stored in the corresponding leaf Q_l.

4.3.2 Contour Merging

A single contour C_{Ql} in Q_l can be complete C^* or incomplete C^+. A complete contour has no further neighboring contours. For each incomplete contour C^+ a connected contour is searched for and a merging procedure follows. It is executed only on the leaf node level in the quadtree and starts with the upper left node. From left to right and top to bottom, connectable contours are searched for in the node's right and bottom neighbors Q_{rb}. The following pseudo code shows the procedure in short.

```
1: for each C₁⁺ in Q_l and C₂⁺ in Q_rb do
2:     if C₁⁺ and C₂⁺ are neighbored
3:         search P_s and P_e in C₁⁺ and split C₁⁺, C₂⁺
4:         merge C₁⁺ and C₂⁺ to C_m
5:         if C_m is a complete contour C*
6:             put C_m into Ω_ZC
7:             remove C₁⁺ and C₂⁺ in Q
8:         else
9:             replace C₁⁺ and C₂⁺ with C_m
10:        end if
11:    end if
12: end
```

First, two merging points are calculated for one incomplete contour C^+ in the current leaf node Q_l (gray quadrant in figure 4). The merging process is executed for this incomplete contour and the incomplete contours of the neighbor leafs Q_{rb} one at a time. The merging start point P_s and end point P_e are calculated by walking clock wise through the points on the contour C^+. P_s represents the most left and bottom point in Q_l that has a matching point on the tile border in Q_{rb}. In a similar way P_e represents the most right and upper point. The points P_s and P_e split the contour C_1^+ and C_2^+ into the contour parts C_i and C_o, respectively C_i' and C_o'. A new contour C_m is created by merging C_o in Q_l with C_o' in Q_{rb}. C_i and C_i' are eliminated. The old contours C_1^+ and C_2^+ are removed and the nodes are updated by linking the merged contour C_m to Q_l and Q_{rb}. If a contour is complete, all links will be removed and the final contour becomes part of Ω_{ZC}. Before adding a contour to Ω_{ZC}, contours that are smaller than a minimum expected zooplank-

ton size have been already eliminated. An illustration of the contour merging can be found in figure 4.
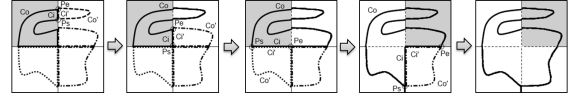

Figure 4: From left to right the contour merging part is illustrated. The gray tile denotes the current leaf node Q_l.

4.4 Pre-classification

The segmented set Ω_{ZC} contains zooplankton and non-zooplankton. The non-zooplankton segments are for example eggs, rotten plankton or other particles. The aim of this step is to classify the elements in the candidate set Ω_{ZC} as one of the three sub-sets:

- reduced zooplankton candidates $\Omega_{ZC'}$
- quasi-round segments Ω_{qr}
- and thin segments Ω_t.

In our scenario the sets Ω_t and Ω_{qr} are typical non-zooplankton. The reduced set $\Omega_{ZC'}$ is produced for the zooplankton recognition resulting in a more stable classification result.

$$\Omega_{ZC'} = \Omega_{ZC} \setminus \{\Omega_{qr}, \Omega_t\} \quad (1)$$

The very fast working algorithms of our approach will be described in the following subsections.

4.4.1 Detection of Quasi-round Segments

Our detection of quasi round segments is simple and fast. Quasi round segments are characterized by a contour shape going from round to quadratic. Eggs and bubbles in the water are quasi round and should not be passed into the recognition step. To be quasi round, an object must exceed a threshold for one of the two following similarities. The similarity to a round shape is calculated from the zooplankton candidate area A_{ZC} and its enclosed circle area A_{ec}. The similarity to a quadratic shape is determined by using the bounding box, whereby the side with the maximal length l is important. The condition for a quasi round object is:

$$\Omega_{qr} = \{C | \forall C \in \Omega_{ZC} : (\frac{A_{ZC}}{A_{ec}} > T_q) \vee (\frac{A_{ZC}}{l^2} > T_r)\} \quad (2)$$

Good thresholds for the detection are $T_q = T_r = 0.6$.

4.4.2 Our Novel Detection of thin Segments

In our case, a thin segment C_t characterizes a filamentous object without big blobs on the inside. Two key

ideas play an important role. The first one is an analysis of the pixel distances to the segment border in a histogram representation. A thin object has a peak in the low distance range of the histogram. The second key idea is to normalize the histogram relative to the radius of a circle with the same area. In comparison to other shapes with the same area, a circle contains the highest distances to the border. An exemplary illustration of the detection approach is pictured in figure 5.
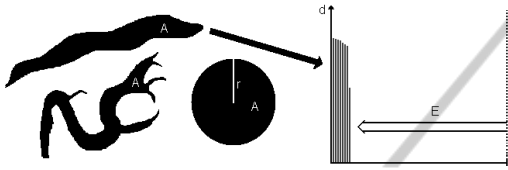

Figure 5: From left to right: Thin objects and a circle with identical areas followed by the corresponding normalized histogram relative to the circle radius with the empty bin amount E are illustrated.

At first, a distance transform is applied on C_t and the area A is calculated. All distances are normalized relative to the radius r of the circle. A second normalization is done, so that $r = 255$. The distances are represented in a histogram with 256 bins. Beginning at the maximal histogram value (255), the empty bins E are counted in direction of the histogram origin. Finally, a threshold T_f is used for the detection as follows:

$$\Omega_t = \{C | \forall C \in \Omega_{ZC} : \frac{E}{255} > T_f\}; \text{ relative to } r = \sqrt{\frac{A}{\pi}} \tag{3}$$

A good threshold for the detection is $T_f = 0.6$.

4.5 Zooplankton Recognition

The recognition is not the major part of our contribution. Nevertheless, we explain it in short to complete the argumentation. In our scenario, the set $\Omega_{ZC'}$ is used for zooplankton species recognition. For every segment 52 features are extracted. The best features are selected by an automatic selection approach. Classification is done with an SVM. The classification result is improved manually by an zooplankton expert with few user interactions. The improved result is stored and used for training an improved classifier.

5 RESULTS

We evaluated the steps chamber segmentation (B), candidate segmentation (C) and pre-classification (D)

separately. The steps (C) and (D) are performed on the results produced with the best method of step (B). All results are compared with ground truth data generated by a zooplankton expert, who analyzed the sample, marked all existing specimen with a bounding box and classified them. For our evaluation five large images with ground truth data were available with following properties:

1. image 1: 62520×62000 pixels, 30×40 tiles

2. images 2,3,4: 64604×66650 pixels, 31×43 tiles

3. image 5: 89612×89900 pixels, 43×58 tiles

5.1 Chamber Segmentation

To evaluate the chamber segmentation, we segmented the chamber in all images manually and compared it to the automatic chamber segmentation results. For the three chamber segmentation methods, we calculate precision, recall and f-score. A value of 1 indicates a perfect segmentation. The standard deviations according to the evaluation measures are illustrated in brackets. The evaluation of the three chamber segmentation methods is presented in table 2.

Table 2: Chamber segmentation evaluation of the longest contour (lc), active contours (ac) and region growing (rg) approach.

	precision	recall	f-score
lc	0.889 (13.5)	0.991 (0.36)	0.927 (8.66)
ac	0.993 (0.14)	**0.997 (0.11)**	0.995 (0.09)
rg	**0.996 (0.17)**	0.995 (0.67)	**0.996 (0.27)**

As can be seen in table 2, the active contour and region growing approach lead to the best results. However, region growing is slightly better. The longest contour approach leads to the worst results with an extracted contour that can be a little bit frayed. Images of the results can be seen in figure 6.
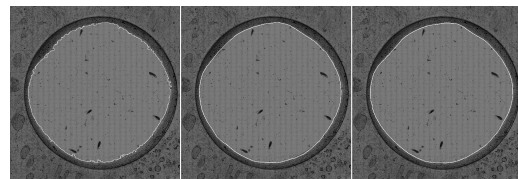

Figure 6: The images show the results of our three approaches for chamber contour detection. From left to right: The longest contour, the active contour and the region growing approach are pictured.

5.2 Zooplankton Segmentation

The segments of the set Ω_{ZC} are compared to the ground truth (manually marked bounding boxes). In Ω_{ZC} are zooplankton and non-zooplankton segments. We only calculate the number of missing zooplankton segments in Ω_{ZC}, because the separation in zooplankton and non-zooplankton segments is done in a later step. In summary, only 0.5% of the ground truth were missing after segmentation.

5.3 Zooplankton Pre-Classification

We evaluate the pre-classification algorithm by comparing the final set $\Omega_{ZC'}$ with the ground truth zooplankton data. For the sets Ω_t and Ω_{qr} an evaluation is only possible by subjective manual estimation. Evaluated by our visual judgment, the sets contain correctly classified thin and quasi round objects (see figure 7).
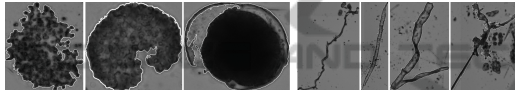

Figure 7: The left images picture quasi round and the right thin objects. The contour of the segment is drawn in white.

The amount of classified segments per image is shown in table 3.

Table 3: Number of segments pre-classified as thin (Ω_t), quasi-round (Ω_{qr}) and zooplankton candidate ($\Omega_{ZC'}$).

image	input	output		
I_{in}	$|\Omega_{ZC}|$	$|\Omega_t|$	$|\Omega_{qr}|$	$|\Omega_{ZC'}|$
1	342	61	27	254
2	361	103	30	228
3	416	71	37	308
4	337	45	39	253
5	644	156	67	421
sum	2100	436	200	1464

The final set $\Omega_{ZC'}$ contains zooplankton and non-zooplankton segments. We evaluate the binary classification case with the measures specificity, precision and recall (see table 4), whereby the best possible value is 1. As can be seen, the specificity and precision of our pre-classification approach is very good,

Table 4: Specificity (sp), precision (pr) and recall (re) of the reduced zooplankton candidate set $\Omega_{ZC'}$

	1	2	3	4	5	All
sp	0.94	0.97	0.97	0.95	0.95	**0.96**
pr	0.96	0.96	0.98	0.97	0.94	**0.96**
re	0.48	0.43	0.40	0.49	0.43	0.44

but the recall is not. In other words, the set $\Omega_{ZC'}$ contains nearly all zooplankton segments, but contains some non-zooplankton segments, too.

6 CONCLUSION AND FUTURE WORKS

We presented a novel approach to segment and pre-classify zooplankton located in a counting chamber in very large images. It is the first approach in the field of zooplankton recognition that is able to deal with images larger than the available main memory of standard computers. We outlined how three different methods can be used to detect the counting chamber and one method to segment the zooplankton with a contour based Split & Merge approach. The segmentation result contains zooplankton and non-zooplankton segments. To reduce the non-zooplankton species, we presented a solution for pre-classifying the segments. The classification algorithm can detect thin and quasi round objects. For the thin object detection, a novel approach was introduced allowing a detection independently of the object shape and rotation. The chamber detection evaluation shows very good results. The evaluation of the zooplankton segmentation and pre-classification show that there are non-zooplankton segments that remain undetected.

Our current work focuses on detecting these non-zooplankton segments by using the segmentation and pre-classification results. We are training one or more classes representing non-zooplankton and we are working on a multi resolution segmentation by using the implemented quadtree. For the recognition we plan to adapt and to develop special shape features like in (Seng, 2013). To extend the system and to be able to segment every zooplankton species without exception an user-driven semi-automatic segmentation like active contours in (Kass et al., 1988) and (Ahmed et al., 2013) is planned.

ACKNOWLEDGEMENTS

REFERENCES

Ahmed, F., Le, H., Olivier, J., and Bon, R. (2013). An active contour model with improved shape priors using fourier descriptors. *VISAPP 2013 - Proceedings of the International Conference on Computer Vision Theory and Applications*, 1:472–476.

Chehdi, K., Boucher, J., and Hillion, A. (1986). Automatic classification of zooplancton by image analysis. In *Acoustics, Speech, and Signal Processing, IEEE International Conference on ICASSP '86.*, volume 11, pages 1477 – 1480.

Culverhouse, P., Williams, R., Simpson, B., Gallienne, C., Reguera, B., Cabrini, M., Fonda-Umani, S., Parisini, T., Pellegrino, F., Pazos, Y., Wang, H., Escalera, L., Moroo, A., Hensey, M., Silke, J., Pellegrini, A., Thomas, D., James, D., Longa, M., Kennedy, S., and del Punta, G. (2006). Hab buoy: a new instrument for in situ monitoring and early warning of harmful algal bloom events. *African Journal of Marine Science*, 28(2):245–250.

Davis, C. S., Gallager, S. M., Bermann, N. S., Haury, L. R., and Strickler, J. R. (1992). The video plankton recorder (vpr): design and initial results. In *Arch. Hydrobiol. Beith.*, volume 36, pages 67–81.

Davis, C. S., Thwaites, F. T., Gallager, S. M., and Hu, Q. (2005). A three-axis fast-tow digital video plankton recorder for rapid surveys of plankton taxa and hydrography. *Limnology and Oceanography-Methods*, 3:59–74.

Dubelaar, G. and Jonker, R. (2000). Cytobuoy: a step forward towards using flow cytometry in operational oceanography. *Sci. Mar.*, 64(2):255–265.

Fawell, J. (1976). Electronic measuring devices in the sorting of marine zooplankton. In *zooplankton fixation and preservation*, pages 201 – 206. Ed. by H.F. Steedman, Paris:UNESCO Press.

Gaston, K. J. and O'Neill, M. A. (2004). Automated species identification: why not? *Philosophical Transactions of the Royal Society of London Series B-Biological Sciences*, 359(1444):655–667+.

Gorsky, G. and Grosjean, P. (2003). Qualitative and quantitative assessment of zooplankton samples. *GLOBEC INTERNATIONAL NEWSLETTER APRIL*, 9.

Herman, A. W. and Dauphinee, T. M. (1980). Continuous and rapid profiling of zooplankton with an electronic counter mounted on a batfish vehicle. *Deep Sea Research Part A. Oceanographic Research Papers*, 27(1):79 – 96.

Jeffries, H., Berman, M., Poularikas, A., Katsinis, C., Melas, I., Sherman, K., and Bivins, L. (1984). Automated sizing, counting and identification of zooplankton by pattern recognition. *Marine Biology*, 78:329–334.

Kass, M., Witkin, A., and Terzopoulos, D. (1988). Snakes: Active contour models. *INTERNATIONAL JOURNAL OF COMPUTER VISION*, 1(4):321–331.

Katsinis, C. (1979). *Digital Image Processing and Identification of Zooplankton*. University of Rhode Island.

Kelkar, D. and Gupta, S. (2008). Improved quadtree method for split merge image segmentation. In *Emerging Trends in Engineering and Technology, 2008. ICETET '08. First International Conference on*, pages 44 –47.

Luo, T., Kramer, K., Samson, S., Remsen, A., Goldgof, D. B., Hall, L. O., and Hopkins, T., editors (2004). *Active learning to recognize multiple types of plankton*, volume 6. IEEE.

Olson, R. J. and Sosik, H. M. (2007). A submersible imaging-in-flow instrument to analyze nano- and microplankton: Imaging FlowCytobot. *Limnology and Oceanography: Methods*, 5:195–203.

Otsu, N. (1979). A Threshold Selection Method from Gray-level Histograms. *IEEE Transactions on Systems, Man and Cybernetics*, 9(1):62–66.

Picheral, M., Guidi, L., Stemmann, L., Karl, D., Iddaoud, G., and Gorsky, G. (2010). The underwater vision profiler 5: An advanced instrument for high spatial resolution studies of particle size spectra and zooplankton. *Limnology and Oceanography: Methods*, 8:462–473.

Samson, S., Hopkins, T., Remsen, A., Langebrake, L., Sutton, T., and Patten, J. (2001). A system for high-resolution zooplankton imaging. *Oceanic Engineering, IEEE Journal of*, 26(4):671 –676.

Seng, L. (2013). Contour-based shape recognition using perceptual turning points. *VISAPP 2013 - Proceedings of the International Conference on Computer Vision Theory and Applications*, 1:487–491.

Sheldon, R. and Parsons, T. R. (1967). *A practical manual on the use of the Coulter counter in marine research*. Coulter Electronics Sales.

Sieracki, C. K., Sieracki, M. E., and Yentsch, C. S. (1998). An imaging-in-flow system for automated analysis of marine microplankton. *Marine Ecology Progress Series*, 168:285–296.

Toth, L. and Culverhouse, P. F. (1999). 3d object recognition from static 2d views using multiple coarse data channels. *Image Vision Comput.*, 17(11):845–858.

Tschepenakis, G., Guigand, C. M., and Cowen, R. K., editors (2007). *Image Analysis Techniques to Accompany a new In Situ Ichthyoplankton Imaging System*. IEEE.

Tschepenakis, G., Guigand, C. M., and Cowen, R. K. (2008). Machine vision-assisted in-situ ichthyoplankton imaging system. *Sea Technology*, 49(12):15–20.

Website (2013a). http://www.fluidimaging.com.

Website (2013b). http://www.hydroptic.com/uvp.html.

Website (2013c). http://www.zooscan.com.